EUROFUSION WPJET1-PR(16) 16147

S Esquembri et al.

Real-time implementation in JET of the SPAD disruption predictor using MARTe

Preprint of Paper to be submitted for publication in
IEEE Transactions on Nuclear Science

This work has been carried out within the framework of the EUROfusion Consortium and has received funding from the Euratom research and training programme 2014-2018 under grant agreement No 633053. The views and opinions expressed herein do not necessarily reflect those of the European Commission.

Real-time implementation in JET of the SPAD disruption predictor using MARTe

S. Esquembri. *Student Member, IEEE,* J. Vega, A. Murari, M. Ruiz, *Member, IEEE,* E. Barrera, *Member, IEEE,* S. Dormido-Canto, R. Felton, M. Tsalas, D. Valcarcel and JET Contributors

***Abstract*— One of the major problems in present tokamaks is the presence of disruptions. If disruptions are not mitigated, they can produce serious damage to the device. Therefore, disruption predictors are needed in order to apply the mitigation techniques in time. In this paper, the real-time implementation in JET of a new type of disruption predictor is presented. The new predictor, Single signal Predictor based on Anomaly Detection (SPAD), does not require past discharges for training purposes. The implementation is based on the Multi-threaded Application Real-Time executor (MARTe) framework. Analysis over all JET's ITER-like Wall campaigns (C28-C34) show that SPAD was able to predict 83.57% of the disruptions with enough time to apply mitigation techniques. The average anticipation time was 389 ms. In this paper the real-time implementation will be discussed, as well as the optimizations developed to make the algorithm suitable for real-time processing. Performance results and possible improvements will also be analyzed.**

***Index Terms*—disruption predictors, fusion experiments, plasma disruptions, real-time processing.**

I. Introduction

Plasma disruptions are one of the major problems in present tokamaks. This phenomenon is currently unavoidable and it produces large thermal loads, strong electro-magnetic (EM) forces, and runaway electrons (RE) that can severely damage the machine components. Disruption detrimental effects scale with the plasma stored energy, and that fact have to be carefully considered in the operation of current tokamaks (like JET, KSTAR, or DIII-D) as well as in the design and development of future tokamaks devices (ITER, DEMO). For example, ITER components are designed mechanically to withstand the EM loads of a certain number of full scale disruptions, but the thermal loads and RE must be properly mitigated to maintain the integrity and longevity of the machine.

Several plasma disruption mitigation techniques have been developed and tested in current fusion devices, as massive gas injection [1, 2], killer pellet injection [3, 4] or Electron Synchrotron Resonance Heating injection [5, 6]. However, these techniques need to be triggered with enough time (>10ms in the JET case) prior to the disruption in order to be effective. This leads to the need of accurate and reliable disruptions predictors. In this context, accuracy and reliability can be defined in terms of detection success rate (>95% required for ITER) and false alarm rate (<5% for ITER). Nevertheless, the physical phenomena leading to plasma disruptions can be only partially explained using complex and non-linear models. This fact makes the development of such predictors very difficult.

With the increase of computational capabilities available in the fusion facilities, different machine learning methods has been used to implement new generation predictors [7-14] with high detection rates. This kind of predictors take as input a set of features obtained from plasma quantities, control signals, or results of processing of the former two. This set is considered a point in a multi-dimensional space that will be divided into two zones: disruptive zone and non-disruptive zone. These predictors require of intense and computationally expensive training with samples of disruptive and non-disruptive discharges in order to effectively split the operational space, and such training samples might not be valid after big changes in the plasma operational space. The more drastic cases of this change are the upgrade of an existing machine and the construction of a new device. But in these cases mitigation techniques still need to be applied from early operation even there is not a discharge database to train the predictors.

In this paper is presented the implementation of a real-time disruption predictor based on signal anomaly detection. The Single signal Predictor based on Anomaly Detection (SPAD) (formerly known as Predictor Based on Outlier Detection (PBOD)) [15-17] learns the normal behavior of a signal from

This work was partially funded by the Spanish Ministry of Economy and Competitiveness under the Projects No ENE2015-64914-C3-1-R, ENE2015-64914-C3-2-R, ENE2015-64914-C3-3-R, predoctoral fellowship BES-2013-064875, and the grant for predoctoral short-term stays in R&D centers (2014). This work has been carried out within the framework of the EUROfusion Consortium and has received funding from the Euratom research and training programme 2014-2018 under grant agreement No 633053. The views and opinions expressed herein do not necessarily reflect those of the European Commission. For JET Contributors, see the Appendix of F. Romanelli et al., Proceedings of the 25th IAEA Fusion Energy Conference 2014, Saint Petersburg, Russia.

S. Esquembri, M. Ruiz, and E. Barrera, are with the Instrumentation and Applied Acoustic Research Group (I2A2), Universidad Politécnica de Madrid, 28031 Madrid, Spain (e-mail: sesquembri@i2a2.upm.es).

J. Vega is with the Laboratorio Nacional de Fusión, CIEMAT, 28040 Madrid, Spain (e-mail: jesus.vega@ciemat.es).

A. Murari is with the Consorzio RFX (CNR, ENEA, INFN, Universitá di Padova, Acciaierie Venete SpA), 35127 Padova, Italy (e-mail: andrea.murari@euro-fusion.org).

S. Dormido-Canto is with the Dpto. Informática y Automática, UNED, 28040 Madrid, Spain (e-mail: sebas@dia.uned.es).

R. Felton, M. Tsalas, and D. Valcarcel are with the EUROfusion Consortium, JET, Culham Science Centre, Abingdon, OX14 3DB, U.K. (e-mail: maximos.tsalas@jet.efda.org).

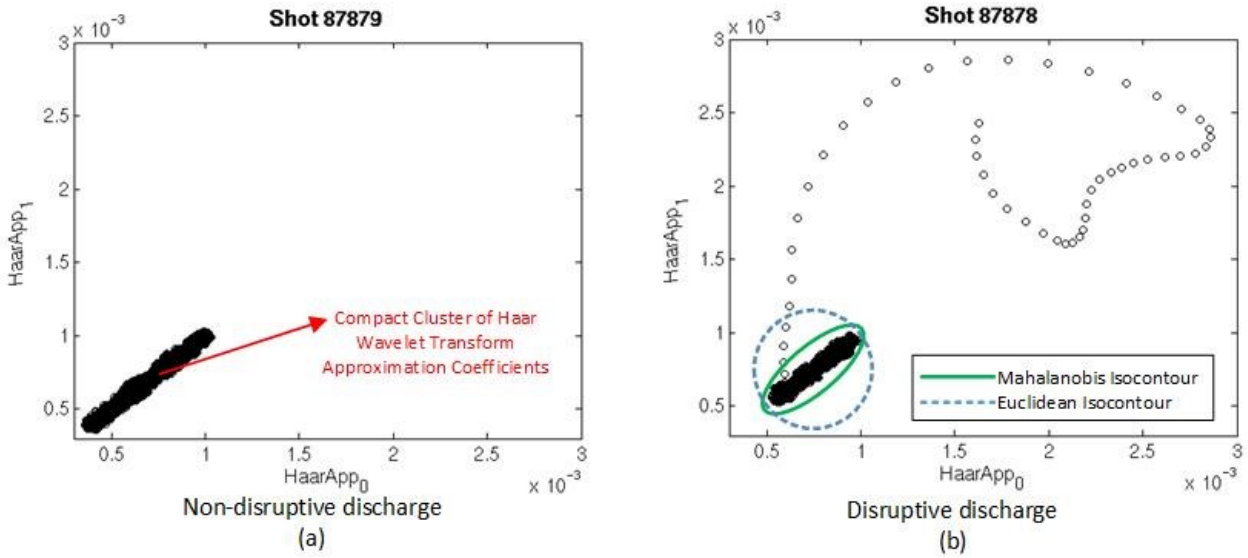

Fig. 1 Representation of the two Haar Wavelet Transform Approximation coefficients for non-disruptive (a) and disruptive (b) discharge as a feature vector in a bidimensional space. Wavelet transform level 4 applied to Locked Mode signal sampled at 1 kHz in 32 sample windows updated every 2 ms. (a) During safe phases of a discharge the vectors are distributed in a compact cluster with positive covariance. (b) Disruptive phases presents outliers with respect the compact cluster. Due to the covariance among the members of the cluster, the outliers can be detected better using the Mahalanobis distance.

the beginning of the discharge, and it triggers the disruption alarm when abnormal behavior is detected. The predictor has been developed using the Multi-threaded Application Real-Time executor (MARTe)[18] framework to be fully integrated into JET Real-Time Data Network (RTDN)[19]. SPAD presents good detection results, comparable with predictors based on machine learning but without the need of training process.

The rest of the paper is organized as follows. First JET's current predictors are presented and discussed. Secondly SPAD predictor is presented, explaining the fundamentals of the algorithm as well as the real-time implementation. Finally, the results are examined and compared to current predictors, followed by the possible enhancements and future work.

II. JET Disruption Predictors

JET is the largest operating tokamak at the moment, and the closest reference to ITER. Experiments taking place in JET will help in the development of ITER. With regard to disruptions, only two kind of disruption predictors are currently implemented in JET: the ones based on threshold cross detection and the Advanced Predictor Of DISruptions (APODIS), based on a Support Vector Machine classifier.

A. Threshold predictors

The threshold based predictors are used upon several plasma signals, as the plasma current, the locked mode (LM) signal, or the restraint ring loop signal. The latter two are used both normalized to the plasma current and non-normalized. This predictor triggers the disruption alarm when the any of the signals crosses a certain threshold. This threshold is set-up individually for each one of the signals. The value is manually chosen prior to the discharges, in a way that the threshold will be lower and more restrictive for discharges with greater potential danger of the possible disruptions produced. Currently these predictors conform the basic disruption predictor system used in JET, used to trigger the disruption mitigation system in all JET discharges. However, this predictor relies on a manually chosen threshold. This method could lead to miss the disruption or detecting it too late if the threshold was set to high, or also to trigger false alarms if the threshold was set too low.

B. APODIS

APODIS predictor is based on Support Vector Machine (SVM) approach. As explained before, machine learning methods, including SVM, are trained using data from past discharges. This training allows the predictor to split the multidimensional feature space formed by signals utilized in the training into safe zone and disruptive zone. APODIS was trained using the data of seven signals (including the LM) of almost 10,000 JET discharges between April 2007 and October 2009 (JET C wall). This training required more than 900h of CPU time in a high performance computer. The success rate of APODIS in the campaigns from C28 to C34 is around 84%.

III. SPAD PREDICTOR

In this section the algorithm implemented will be briefly explained as well as MARTe, the framework used for its implementation and integration in JETs RTDN. After that, the implementation of each of the algorithm steps will be explained in detail, including the optimizations and parametrizations implemented.

A. Algorithm description

As mentioned before, SPAD predictor detects abnormal behavior in a signal to trigger the disruption alarm. More precisely, SPAD uses one of the signals also used for threshold based disruption prediction, the LM signal. This signal is closely related with the disruptive behavior and the predictor shows a good relation between anomalies in the

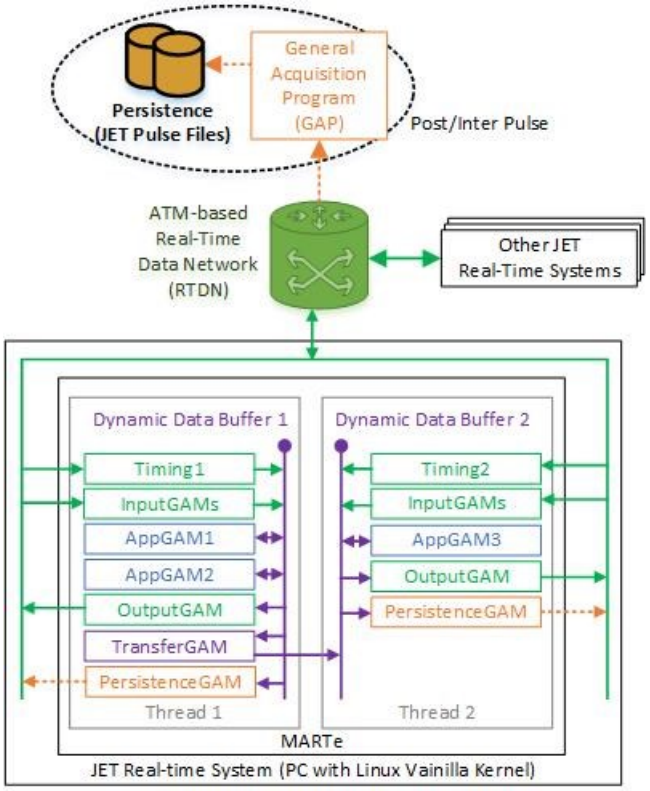

Fig. 2 Schema of typical MARTe application and its integration into JETs RTDN and persistence system.

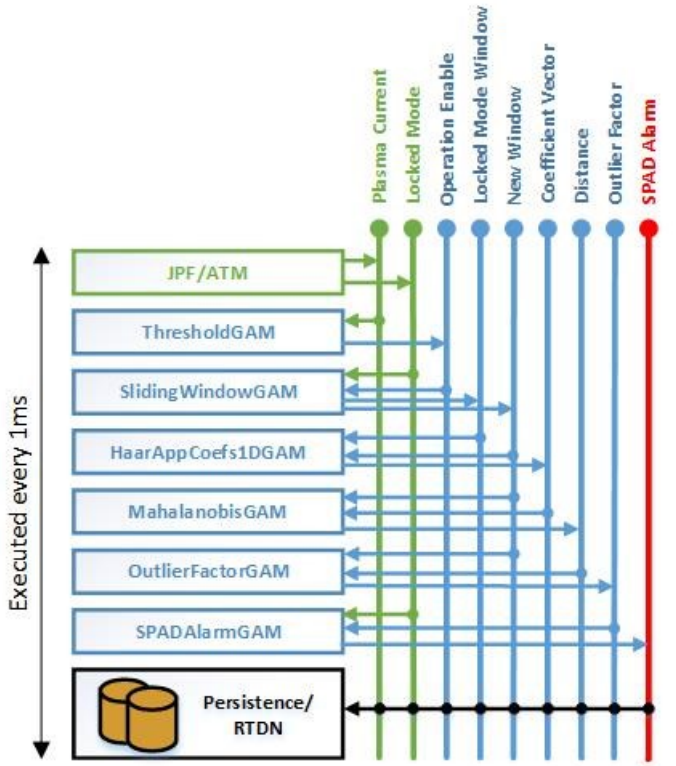

Fig. 3 Diagram of SPAD implementation in MARTe. GAMs are executed in order from top to bottom.

signal and the disruptions. The LM signal is read every 1ms and the latest 32 samples are processed every 2ms. The predictor uses the time and frequency information of the LM obtained by means of a wavelet transform. In particular, the approximation coefficients of the Haar Wavelet transform are used. These coefficients are used as a feature vector. The representation of this vector as a point in a multidimensional space shows that in non-disruptive discharges and in the non-disruptive phases of a disruptive discharge the feature vectors are distributed in a compact cluster, while in the disruptive phase of a discharge this vectors are far from the original cluster. Fig. 1 shows the representation of these vectors for the case of two dimensional feature vectors. Due to the obvious positive covariance present among the feature points of the cluster, the Mahalanobis distance method was chosen to measure the distance of a point with respect to the centroid of the cluster. Finally, an outlier factor is calculated using statistical measures of the Mahalanobis distance during the discharge as standard deviation and mean. The disruption alarm will be raised when the outlier factor surpasses a certain threshold. Analysis over all JETs ITER-like Wall (ILW) campaigns show good detection results when setting this threshold to 10 for all the discharges.

B. MARTe

MARTe is a framework originally developed for JET real-time applications and now in use in several fusion devices as RFX, COMPASS, ISTTOk, and FTU [20-22]. The main objective of MARTe is to abstract an implementation from the plant hardware and software interface with plant input/output system. It also provides tools for real-time thread scheduling, offline and online validation, and an architecture allowing code reuse and easy maintainability.

MARTe applications consist of a set of Generic Application Modules (GAMs) connected by means of the Dynamic Data Buffer (DDB). Each GAM can read and write an arbitrary number of data from the DDB. Special GAMs might be used to perform Input/Output task, as sample signals from the RTDN or send the alarm value to the RTDN. GAMs are executed inside threads managed by the real-time scheduler. Communication and synchronization between the GAMs executed in different threads is also possible. An example of a MARTe application structure and how are they integrated with JETs RTDN and persistence system is depicted in Fig. 2. The number of threads, their timing, or the distribution of GAMs among the threads is completely configurable. In runtime, the real-time executor will run periodically the GAMs of each thread in the order specified.

This architecture allows the modularization of an algorithm in a set of GAMs, each one of them can be easily reused in other application. Modifications of a specific GAM (e.g. for improve the performance) are also possible and can be done without modifying the rest of the GAMs as long as the interface (the DDB data read and write) still invariable.

C. SPAD GAMS

The implementation of the SPAD predictor for MARTe is depicted in Fig. 3. This implementation required the development of six GAMS: ThresholdGAM,

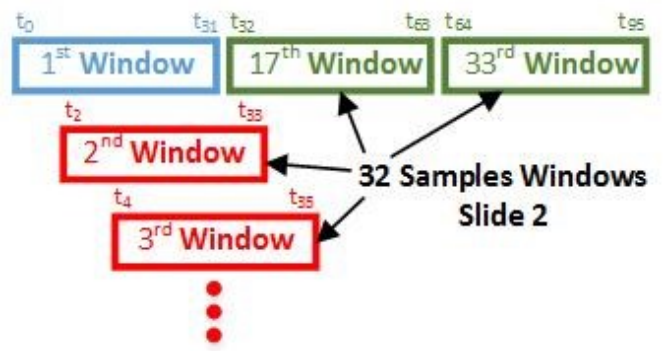

Fig. 4 Explanation of packaging signal samples in sliding windows. Example of the distribution of samples in windows of 32 elements sliding each 2 elements.

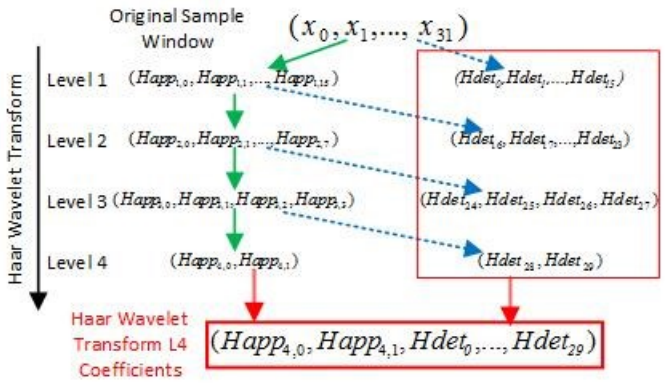

Fig. 5 Explanation of the process for obtaining Haar Wavelet Transform coefficients over several iterations of the transform. In SPAD, only the approximation coefficients will be used.

SlidingWindowGAM, HaarAppCoef1DGAM, MahalanobisGAM, OutlierFactorGAM, and SPADAlarmGAM. It also uses standard MARTe GAMs for reading the plasma current and locked mode signals from the RTDN as well as writing the alarm value also in the RTDN. In the verification and validation phase these signals were read from JETs Pulse Files (JPFs). JPFs will be also used to store all the intermediate data used in the algorithm for future analysis of the predictor behavior. All these GAMs are executed sequentially in a single thread. As in the original algorithm the LM signal is read every 1ms, the thread and therefore all SPADs GAM must be processed in less than 1ms. One important thing to mention is that every GAM configuration detailed in the next sub-sections is done in the initialization phase, and it cannot be changed in runtime. That allows to perform some calculations and all the memory allocation in the start-up phase.

1) ThresholdGAM

This GAM controls that the rest of GAMs do not perform any operation until the initial phase of the plasma has finished. The reason behind this is that the value of the LM signal can have strange behavior at the beginning of a discharge. The startup phase is considered finished once the plasma current reaches a certain configurable threshold, typically 750kA. Therefore, this GAM just compare the input value with a configurable threshold and enable an output signal to the DDB when the condition is met. This output will be an input for the rest of the GAMS, which will do nothing but reset themselves to the initial status when the signal is disabled.

2) SlidingWindowGAM

This GAM will produce the input for the Haar Wavelet transform. The GAM stores the input internally, in this case the LM signal, and produces an output with a set of the latest values of the signal. This set of values will be called "window". Both the size of the window (i.e. the number of latest values returned) and the update rate of the window (i.e. the slide) are completely configurable. A secondary output named "New Window" will be enabled when a new window is available. For the implementation of SPAD, the GAM is configured with a window size of 32 elements updated every 2 cycles. Fig.4 shows an example of how the signal will be grouped in these sliding windows. As the thread is executed every 1ms, the SlidingWindowGAM will produce a new window every 2ms containing the latest 32 samples of the LM signal, or what is the same, the values of the LM signal during the last 32ms reading the latest value of the signal every 1ms.

3) HaarApp1DCoefGAM

This GAM will calculate the Haar Wavelet transform approximation coefficients of each new window returned by the SlidingWindowGAM. The application of the Haar Wavelet transform (H) to an even vector X of size n produces n coefficients, being the half of them approximation coefficients (H_{App}) and the other half detail coefficients (H_{Det}) as shown in the equation (1).

$$\begin{aligned} &X[k] = (x_0[k], \ldots, x_{n-1}[k]) \\ &\mathrm{H}(X[k]) = H[k] = (H_{App}, H_{Det}) = \\ &\quad = ((H_{App,0}[k], \ldots, H_{App,n/2}[k]), (H_{Det,0}[k], \ldots, H_{Det,n/2}[k])) \\ &H_{App,i}[k] = \sqrt{2}(x_{2i} + x_{2i+1})/2 \qquad H_{Det,i}[k] = \sqrt{2}(x_{2i} - x_{2i+1})/2 \end{aligned} \tag{1}$$

The same operation can be performed successively over the approximation coefficients to obtain the transform next level coefficients. Fig. 5 shows how the Haar Wavelet transform is applied to a vector of 32 elements to obtain the level 4 coefficients. The HaarApp1DCoefGAM calculates the Haar Wavelet transform approximation coefficients for any even-sized input array. The transformation level applied is configurable but it must be take into account that the next level of the transform can only be applied if the number of previous level approximation coefficients is even. This condition is checked at the GAM initialization phase. To reduce the computational effort, the details coefficients are not calculated, and the approximation coefficients are calculated in one step instead of applying consecutively (1).

4) MahalanobisGAM

This GAM calculates the Mahalanobis distance between the current feature vector and the centroid of all past feature vectors in a multidimensional space. The Mahalanobis distance (D_M) is defined as (2).

TABLE I
SPAD DETECTION RATES COMPARISON USING DIFFERENT FEATURE VECTOR SIZE

Feature Vector Size	False Alarms	Missed Alarms	Tardy Detections	Valid Alarms	Premature Alarms
16	18.24%	11.31%	3.00%	79.68%	6.01%
8	8.98%	10.60%	3.18%	83.57%	2.65%
4	9.55%	10.95%	3.36%	82.86%	2.83%
2	9.84%	11.31%	3.53%	81.98%	3.18%

$$D_M[k]=\sqrt{(H_{App}[k]-\mu(H_{App}[0..k-1]))^T\Sigma^{-1}(H_{App}[k]-\mu(H_{App}[0..k-1]))} \quad (2)$$

In this case, the feature vector used as input will be the vector containing the Haar approximation coefficients (H_{App}). This equation includes the mean (μ) and the covariance matrix ($\sum$) of a set of feature vectors which number increase during the discharge. If the mean vector and the covariance matrix were calculated from scratch each cycle, not only the memory but also the computation time will increase each cycle, making the implementation not suitable for long discharges. Instead of that, partial sums and products are stored in such a way that both the computation time and the memory usage scale only with the size of the feature vector and remains bounded for all the discharge. This optimization was carefully reviewed and tested as this kind of operations can induce rounding errors.

5) OutlierFactorGAM

This GAM calculates the outlier factor (O_F) of the current feature vector using (3). Similar to the MahalanobisGAM, the standard deviation (σ) and mean (μ) appearing in (3) must be calculated with respect to the set of all previous Mahalanobis distance values in the discharge. The approach implemented in this GAM is comparable with the one in MahalanobisGAM, consisting in the storage of partial sums and products in order to make the execution time independent of the number of Mahalanobis distances previously calculated.

$$O_F[k]=\left|\frac{(D_M[k]-\mu(D_M[0..k-1]))}{\sigma(D_M[0..k-1])}\right| \quad (3)$$

6) SPADAlarmGAM

This GAM triggers the alarm in case of anomaly detection. The anomaly is detected when the outlier surpasses a configurable threshold at the same moment that the LM signal reaches a global maxima. Therefore, this GAM must keep the current LM global maxima as well as compare the current outlier factor with the configured threshold.

IV. RESULTS

The presented implementation has been validated using the data from all JETs safe and unintentional disrupted discharges in the range of 82460-87918. These correspond to all JET campaigns with the ILW from 2011 to 2014. This set contains 566 unintentional disruptive discharges and 1738 safe discharges. The comparison of the detection results of the real-time MARTe implementation and an equivalent implementation in MATLAB free of optimizations showed that the optimizations did not affect the behavior of the triggered alarm. The test environment for the validation was a computer with an i7 4790 (4 cores, 2 threads/core, 3.6 GHz) CPU and 16 GB of RAM running a Red Hat Enterprise Linux 6.5 with a Vanilla Linux Kernel. In the validation, each discharge was simulated using LM and plasma current data obtained from JPFs. For all the discharges, the GAMs where configured as follows. The plasma current threshold to start the predictor was 750 kA. The latest available value of LM signal was read every 1 ms and processed every 2ms in time windows containing the latest 32 samples. Several Haar Wavelet transform levels were tested, including from level 1 (16 approximation coefficients) to level 4 (2 approximation coefficients). The outlier factor threshold was set to 10 for all the discharges.

TABLE II
SPAD, APODIS, AND LMPT DETECTION RATE COMPARISON

Predictor	False Alarms	Missed Alarms	Tardy Detections	Valid Alarms	Premature Alarms
SPAD	7.42%	10.60%	3.18%	83.57%	2.65%
APODIS	<5%	15.38%	2.47%	79.15%	3.00%
LMPT	---	30.39%	3.00%	63.69%	2.65%

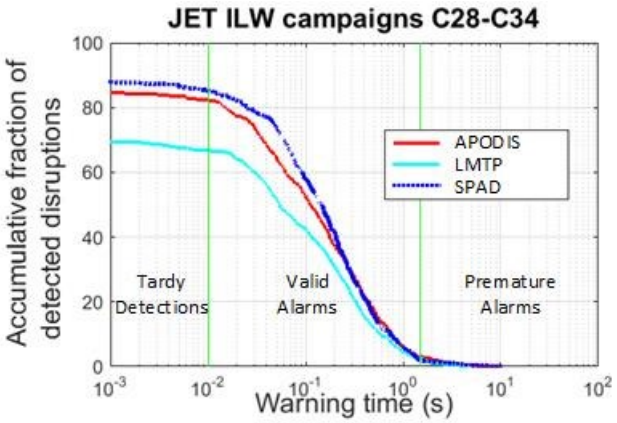

Fig. 6 Representation of the accumulative fraction of detect disruptions with regard to total disruptions during all JETs ILW campaigns.

A. Detection results

Table I shows the detection results for the configuration described above. Disruption detections triggered 1.5 s before the disruption are considered "Premature alarms", as they are not considered true predictions. "Valid alarms" are considered those which were triggered between 1.5 s and 10 ms, as 10 ms is the minimum time to apply properly the disruption mitigation techniques. "Tardy detections" are those triggered with less than 10 ms in advance, as is already too late to apply the mitigation techniques properly. If the alarm was trigger after the disruption or was not triggered at all in a disruptive discharge is considered a "Missed alarm". Those cases where the alarm is triggered and no disruption occur are classified as "False alarms". False alarms are an important issue, as the

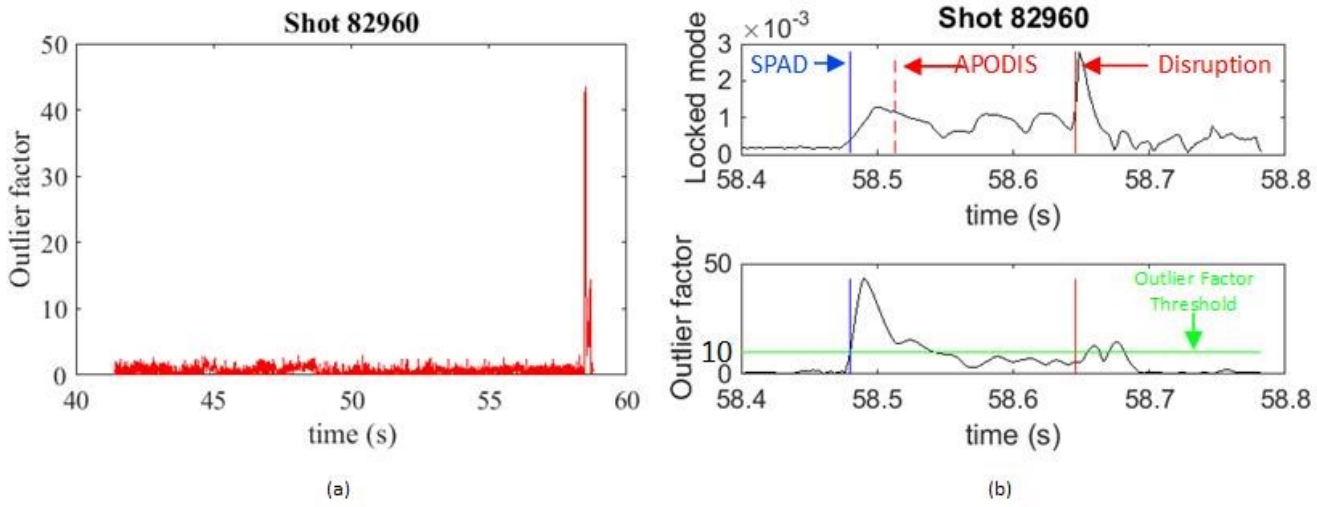

Fig. 7 Representation of the behavior of SPAD outlier factor in the discharge 82960. (a) shows the value of the outlier factor during the whole discharge. (b) depict the comparison between Locked Mode signal and the outlier factor moments before the disruption as well as the moment when SPAD and APODIS predict the disruption. LMPT missed this disruption.

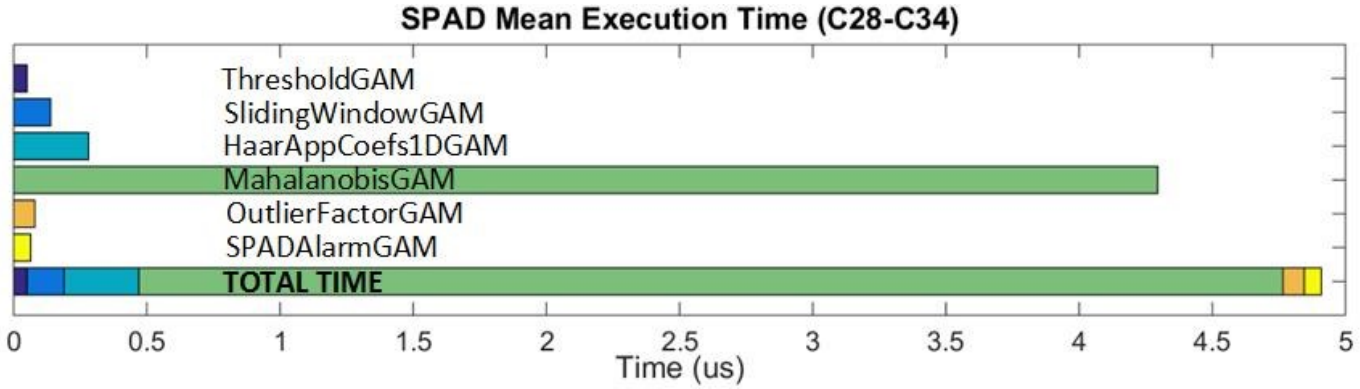

Fig. 8 SPAD GAM average cycle execution time for a confidence level of 97%. The execution time confidence level is given by adding three times the standard deviation to the mean. The test set was all JET safe and non-intentional disruptive discharges with ITER-like Wall (C28-34). The test computer consist of a i7 4790 (4 cores, 2 threads/core, 3.6 GHz) with 16 GB of RAM running an Red Hat Enterprise Linux 6.5. In the chart can be observed that the total cycle execution time is far from the maximum allowed for the proper execution of the algorithm (1 ms).

triggering of the mitigation techniques will end with the discharge. In that cases, if SPAD was directly connected to the disruption mitigation systems, this false alarms would have ended safe plasma discharges prematurely without reason, with the waste of time and resources that comes along.

Table II and Fig. 6 represents the comparison of SPAD with Locked Mode Predictor based on a Threshold criterion (LMPT) and APODIS using the same classification criteria. With more than 83% of valid alarms, SPAD slightly outperforms APODIS detection results (79.15%), while LMPT remains with only 63.96% of valid alarms.

Fig.7 (a) shows the evolution of the SPAD outlier factor for the disruptive discharge 82960. There can be observed that the outlier value remains very low until the very end of the discharge, when the disruption occurred. In Fig.7 (b) the values of the LM signal and the outlier factor are shown in detail, including SPAD and APODIS detection time. LMPT missed this disruption because the increase in the LM signal occur very close to the disruption and the threshold was set too high.

B. Execution time and computational complexity

The execution time was measured using MARTe tools. Fig.8 shows a breakdown by GAMs of the average cycle execution time for all the test set with a confidence level of 97%. The confidence level is given by adding to the mean time value three times the standard deviation. The GAM requiring more execution time is the MahalanobisGAM, what is reasonable due to the calculation of inverse covariance matrix and the vector-matrix-vector multiplication needed to obtain the Mahalanobis distance. The maximum execution time measured during this analysis was 26.9280 us. This big difference between mean and maximum time can be explained with operative system interruptions, as the test platform was not running a real-time operative system. Other reason contributing to this difference is the calculation of the inverse covariance matrix in the MahalanobisGAM, as this is solved using the LUP-factorization.

V. Conclusions and Future Work

A real-time disruption predictor has been successfully

implemented using MARTe framework. The use of this framework allows the easy integration in JETs RTDN. The validation of the algorithm against all JETs safe and unintentionally disrupted discharges with the ITER-like Wall reveal better prediction results (83.57% of valid alarms) than APODIS and LMTP. Several optimizations were developed with respect to the original algorithm for making the execution time dependent only of the dimensionality of the problem and not of the pulse duration. The implemented algorithm do not need data from previous discharges, what can be very useful for new devices, after an upgrade in an existing machine, and when the plasma operation parameter changes drastically. Other important fact is that there is no need of change the configuration depending on the discharge characteristics. The performance of the algorithm have been measured in a test environment, probing its suitability for a real-time system.

Among the possible improvements for the predictor, one of the most important is to reduce the number of false alarms. Currently there is work been done to identify the causes of these false detections and decrease its number at least to the percentage estimated valid for ITER (<5%). However, disruptions can heavily damage the machine, and SPAD could have save the machine from numerous disruptions not detected by the LMPT.

Other line of work currently active is the identification of more signals to be added in the SPAD algorithm. The addition of relevant signals related with the root causes of the disruption could improve the detection results or reduce the false alarm ratio. Other possible enhancement it is the estimation of the optimal threshold for the outlier factor dynamically during the discharge.

With respect to the execution time, the current implementation is good enough for the process of one signal with the extraction of 8 Haar approximation coefficients. Nevertheless, the addition of a second or third signal with its corresponding approximation coefficients could make the dimensionality of the covariance matrix too big for the current implementation, not been able to process it in less than 1 ms. To solve this, better approaches for the calculation of the inverse matrix and the vector-matrix-vector product required by the Mahalanobis distance can be studied and implemented.

REFERENCES

[1] M. Lehnen, A. Alonso, G. Arnoux, N. Baumgarten, S. A. Bozhenkov, S. Brezinsek, M. Brix, T. Eich, S. N. Gerasimov, A. Huber, S. Jachmich, U. Kruezi, P. D. Morgan, V. V. Plyusnin, C. Reux, V. Riccardo, G. Sergienko, M. F. Stamp and J. E. contributors, "Disruption mitigation by massive gas injection in JET," Nucl Fusion, vol. 51, pp. 123010, 2011.

[2] M. Bakhtiari, G. Olynyk, R. Granetz, D. G. Whyte, M. L. Reinke, K. Zhurovich and V. Izzo, "Using mixed gases for massive gas injection disruption mitigation on Alcator C-Mod," Nucl Fusion, vol. 51, pp. 063007, 2011.

[3] N. Commaux, L. R. Baylor, S. K. Combs, N. W. Eidietis, T. E. Evans, C. R. Foust, E. M. Hollmann, D. A. Humphreys, V. A. Izzo, A. N. James, T. C. Jernigan, S. J. Meitner, P. B. Parks, J. C. Wesley and J. H. Yu, "Novel rapid shutdown strategies for runaway electron suppression in DIII-D," Nucl Fusion, vol. 51, pp. 103001, 2011.

[4] G. Pautasso, K. Buchl, J. C. Fuchs, O. Gruber, A. Herrmann, K. Lackner, P. T. Lang, K. F. Mast, M. Ulrich and H. Zohm, "Use of impurity pellets to control energy dissipation during disruption," Nucl Fusion, vol. 36, pp. 1291, 1996.

[5] B. Esposito, G. Granucci, P. Smeulders, S. Nowak, J. Martin-Solis and L. Gabellieri, "Disruption avoidance in the Frascati Tokamak Upgrade by means of magnetohydrodynamic mode stabilization using electron-cyclotron-resonance heating," Phys. Rev. Lett., vol. 100, pp. 045006, 2008.

[6] B. Esposito, G. Granucci, M. Maraschek, S. Nowak, A. Gude, V. Igochine, E. Lazzaro, R. McDermott, E. Poli, J. Stober, W. Suttrop, W. Treutterer, H. Zohm, D. Brunetti and A. U. Team, "Avoidance of disruptions at high Î² N in ASDEX Upgrade with off-axis ECRH," Nucl Fusion, vol. 51, pp. 083051, 2011.

[7] B. Cannas, A. Fanni, E. Marongiu and P. Sonato, "Disruption forecasting at JET using neural networks," Nucl Fusion, vol. 44, pp. 68, 2003.

[8] B. Cannas, R. Delogu, A. Fanni, P. Sonato, M. Zedda and JET-EFDA contributors, "Support vector machines for disruption prediction and novelty detection at JET," Fusion Eng. Des., vol. 82, pp. 1124-1130, 2007.

[9] J. M. Lopez, J. Vega, D. Alves, S. Dormido-Canto, A. Murari, J. M. Ramirez, R. Felton, M. Ruiz and G. de Arcas, "Implementation of the Disruption Predictor APODIS in JET's Real-Time Network Using the MARTe Framework," IEEE Trans. Nucl. Sci., vol. 61, pp. 741-744, APR, 2014.

[10] A. Murari, G. Vagliasindi, P. Arena, L. Fortuna, O. Barana, M. Johnson and JET-EFDA Contributors, "Prototype of an adaptive disruption predictor for JET based on fuzzy logic and regression trees," Nucl Fusion, vol. 48, pp. 035010, 2008.

[11] G. Pautasso, S. Egorov, C. Tichmann, J. C. Fuchs, A. Herrmann, M. Maraschek, F. Mast, V. Mertens, I. Perchermeier, C. G. Windsor and T. Zehetbauer, "Prediction and mitigation of disruptions in ASDEX Upgrade," J. Nucl. Mater., vol. 290–293, pp. 1045-1051, 3, 2001.

[12] G. Rattá, J. Vega, A. Murari and JET-EFDA Contributors, "Improved feature selection based on genetic algorithms for real time disruption prediction on JET," Fusion Eng. Des., vol. 87, pp. 1670-1678, 2012.

[13] J. Vega, S. Dormido-Canto, J. M. López, A. Murari, J. M. Ramírez, R. Moreno, M. Ruiz, D. Alves and R. Felton, "Results of the JET real-time disruption predictor in the ITER-like wall campaigns," Fusion Eng. Des., vol. 88, pp. 1228-1231, 10, 2013.

[14] M. Versaci and F. C. Morabito, "Fuzzy time series approach for disruption prediction in Tokamak reactors," Magnetics, IEEE Transactions On, vol. 39, pp. 1503-1506, 2003.

[15] J. Vega, R. Moreno, A. Pereira, S. Dormido-Canto, A. Murari and J. Contributors, "Advanced disruption predictor based on the locked mode signal: Application to jet," in Proceedings of the 1st EPS Conference on Plasma Diagnostics (ECPD2015). 14-17 April 2015. Frascati, Italy. Online at Http://Pos. Sissa. it/Cgi-Bin/Reader/Conf. Cgi? Confid= 240, Id. 28, 2015, pp. 28.

[16] J. Vega, A. Murari, S. Dormido-Canto, R. Moreno, A. Pereira, G. A. Rattá and JET Contributors, "Disruption precursor detection: Combining the time and frequency domains," in 26th Symposium on Fusion Engineering (SOFE 2015), Austin (TX), USA, 2015, .

[17] J. Vega, A. Murari, S. Dormido-Canto, R. Moreno, A. Pereira, and S. Esquembri, "Real-time anomaly detection for disruption prediction: the JET case," Nucl. Fusion, Paper NF-101126.

[18] A. C. Neto, F. Sartori, F. Piccolo, R. Vitelli, G. De Tommasi, L. Zabeo, A. Barbalace, H. Fernandes, D. F. Valcárcel and A. J. Batista, "MARTe: a multiplatform real-time framework," Nuclear Science, IEEE Transactions On, vol. 57, pp. 479-486, 2010.

[19] R. Felton, K. Blackler, S. Dorling, A. Goodyear, O. Hemming, P. Knight, M. Lennholm, F. Milani, F. Sartori and I. Young, "Real-time plasma control at JET using an ATM network," in Real Time Conference, 1999. Santa Fe 1999. 11th IEEE NPSS, 1999, pp. 175-181.

[20] F. Janky, J. Havlicek, D. Valcarcel, M. Hron, J. Horacek, O. Kudlacek, R. Panek and B. Carvalho, "Determination of the plasma position for its real-time control in the COMPASS tokamak," Fusion Eng. Des., vol. 86, pp. 1120-1124, 2011.

[21] G. Manduchi, A. Luchetta, A. Soppelsa and C. Taliercio, "The new feedback control system of RFX-mod based on the MARTe real-time framework," Nuclear Science, IEEE Transactions On, vol. 61, pp. 1216-1221, 2014.

[22] A. C. Neto, D. Alves, L. Boncagni, P. J. Carvalho, D. F. Valcárcel, A. Barbalace, G. De Tommasi, H. Fernandes, F. Sartori and E. Vitale, "A survey of recent MARTe based systems," Nuclear Science, IEEE Transactions On, vol. 58, pp. 1482-1489, 2011.